

# ABLATION OF CARBON/CARBON COMPOSITES: 3D MULTI-SCALE SIMULATION OF SURFACE ROUGHNESS EVOLUTION.

Jean Lachaud<sup>1</sup>, Gérard Vignoles<sup>1</sup>, Yvan Aspa<sup>1</sup>, and Jean-François Epherre<sup>1,2</sup>

<sup>1</sup>Laboratoire des Composites ThermoStructuraux (LCTS)  
UMR 5801: CNRS-SAFRAN-CEA-UB1

Domaine Universitaire de Bordeaux – 3, Allée de La Boétie, 33600 Pessac, France  
Corresponding author : jean.lachaud@gadz.org

<sup>2</sup>CEA-CESTA, 33114 Le Barp, France

## Abstract

This work aims to explain and model the complex behavior of carbon-carbon composites during ablation; a special emphasis is set on the onset of surface roughness which induces a strong enhancement of heat and mass transfer and increases ablation effects. The multi-scale surface roughness of a carbon-carbon composite ablated in an oxidation reactor is first analyzed by SEM, micro-tomography and TEM. It is proved to be strongly correlated to the heterogeneity of the composite with respect to heterogeneous mass transfer. Accordingly, the proposed models are based on the simultaneous resolution of a gas diffusion-reaction equation and of a surface evolution equation.

The multi-scale modeling includes two parts. First, using the results of a previous work, the ablation behavior of the perpendicular bundles is modeled in steady state to infer its effective behavior. Then, the overall composite structure is modeled in 3D in transient regime. The input values are either experimental (inter-bundle matrix) or deduced from the first change of scale (perpendicular yarn) or obtained by identification using an inverse method (parallel yarn). At each scale, the models are validated by comparison to experiments in an oxidation reactor.

The mathematical structure of the models and their morphological results are known to be the same when the cause of ablation is either sublimation or oxidation. Then, the results of the models can help understanding the ablation of C/C composites in plasma-jet tests or real flight experiments, at least from the material point of view. Indeed, they prove that from the study of the surface morphology, it is possible to deduce by inverse analysis the properties of the elements in the test conditions.

Key words: Ablation, Modeling, Carbon-carbon composites, Surface Roughness, Design applications.

## 1. INTRODUCTION

The design of thermal protection systems relies on Carbon/Carbon (C/C) composites, which keep excellent mechanical properties at high temperature [1]. However, a high interfacial mass transfer leads to surface recession. C/C composites are progressively destroyed by oxidation and sublimation. These physico-chemical phenomena, collected in the term *ablation*, are globally endothermic. Hence, they are partially beneficial as they reduce the wall temperature and the heat flux that penetrates the internal structure [2].

Ablation of C/C composites leads to a typical surface roughness which induces an enhancement of heat and mass transfer between the protection wall and the surrounding environment via two major phenomena: (i) it increases

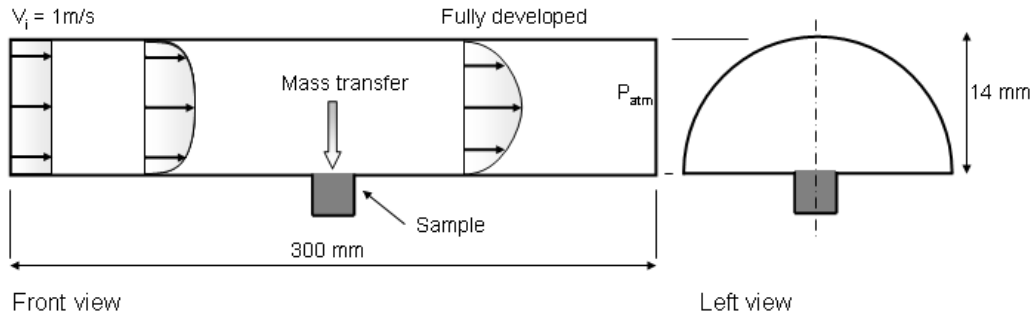


Figure 1. Oxidation reactor geometry and experimental conditions (dry air at  $T = 625^{\circ}\text{C}$ ,  $P = 1\text{atm}$ ).

the chemically active surface of the wall; (ii) it contributes to the laminar-to-turbulent transition in the dynamic boundary layer. PANT program results shows that the heat flux may be multiplied by a factor up to three in turbulent regime [3]. The obvious consequence is a considerable enhancement of global ablation velocity.

If general phenomenological tendencies are now well explained and simulated in the bulk fluid phase [4, 5], the understanding of the interaction between the material and the flow close to the wall has to be improved. In this work, the emphasis is set on surface roughness analysis and modeling for a carbon/carbon composite (C/C). First, a morphological analysis of multi-scale roughness features is briefly presented for this material. Second, the causes of surface roughness onset are discussed. Then, a reaction-diffusion and moving interface model, already presented in details in a previous work [6], is summarized. Using this model two changes of scales are performed to explain the multi-scale behavior of C/C. At each scale, the results are compared to experimental observations for validation or exploitation. In the concluding remarks, several potential applications of the model for the design of thermal protections are presented.

## 2. ANALYSIS OF SURFACE ROUGHNESS

### 2.1. Description of the ablation test

C/C composite samples have been ablated in a cylindrical oxidation reactor at a controlled temperature ( $625^{\circ}\text{C}$ ) under dry air at atmospheric pressure. The reactor section is a  $14\text{ mm}$  diameter half-disk. Its effective length is  $30\text{ cm}$ . The sample is reduced to a  $1\text{ cm}^2$  square surface incorporated in the center of the lower wall of the reactor (see figure 1). The average velocity of the flow is  $1\text{ m}\cdot\text{s}^{-1}$ . This value has been chosen to ensure a high laminar oxygen injection flow. The global scale modeling of the reactor is addressed in an other work; the model has been solved using Fluent 6 [7]. The Péclet mass number close to the sample has been shown to be low, *i.e.* the advection velocity close to the sample is negligible when compared to the mass diffusion velocity. The dynamic boundary layer is not fully developed on the sample; this enables a larger mass transfer by diffusion. These conditions promote a reaction limited mass transfer in the bulk fluid phase.

This unconventional ablation test has three main interests for the first steps into surface roughness modeling: (i) it provides isothermal conditions on the sample, (ii) advection is negligible close to the wall, and (iii) the rough morphologies observed are quite similar to the morphologies obtained with plasma jet tests (see subsection 2.2).

### 2.2. C/C analysis

The studied material is a 3D C/C composite, made from a 3D ex-PAN carbon fibre preform and a pitch-based carbon matrix. It is a heterogeneous multi-scale material. Several thousands of fibers are linked together into a unidirectional bundle with a pitch-based matrix. Then, bundles are orthogonally fit together into a pattern repeated

by translation on a cubic lattice. This macrostructure leads to a network of parallelepipedic macropores (located near each node of the lattice), which are partially filled with pitch matrix. The composite has then been graphitized.

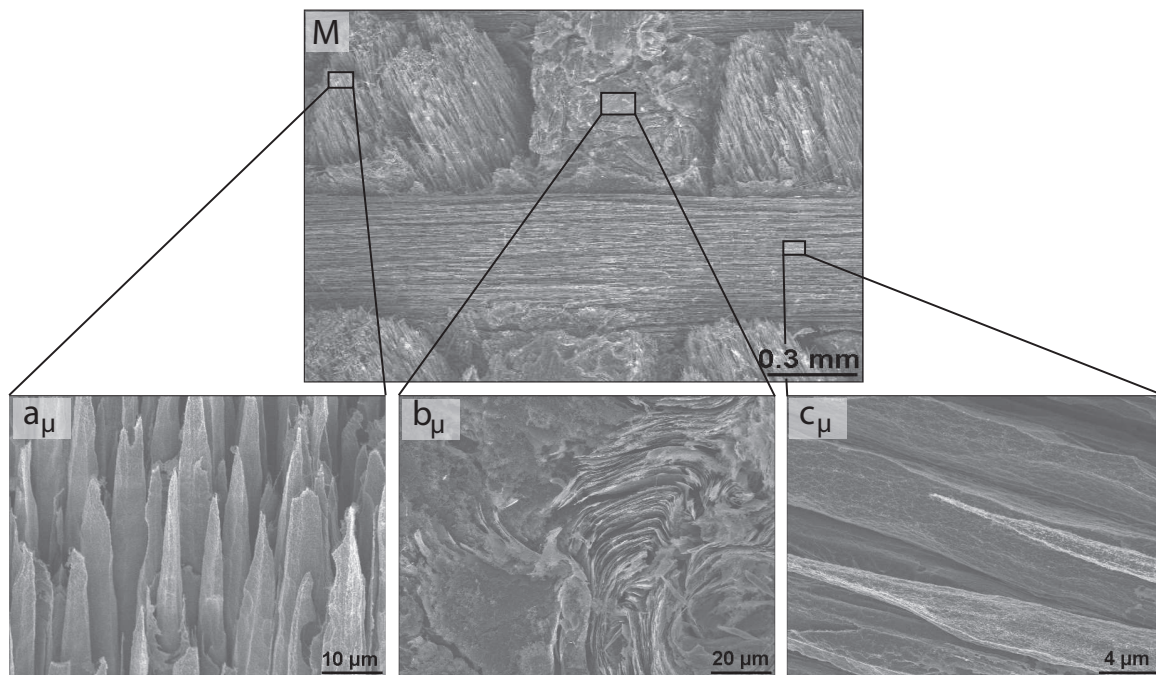


Figure 2. SEM micrographs of 3D C/C surface after ablation in an oxidation reactor

The surface roughness of the ablated C/C composite has mainly been observed by scanning electron microscopy (SEM) and phase-contrast X-ray microtomography (CMT). The micrographs of figure 2 illustrate the multi-scale surface roughness [8]:

- A macroscopic surface roughness takes place on the lattice of the composite (micrograph  $M$ ). It seems to result from the difference of reactivity between bundles and extra-bundle pitch-based matrix. Notches appear between emerging bundles. The section of the bundles emerging perpendicularly to the surface are conical. On the tip of the cone, a plateau appears. The presence of this plateau, relevant of the transient regime, will be discussed in the model results. The bundles which are parallel to the surface are not rough at this scale but their surface is slightly undulated in their cross section.
- A mesoscopic surface roughness develops at the end of emerging bundles, and looks like "needle clusters" (micrograph  $a_{\mu}$ ) -resp. "needle layers" (micrograph  $c_{\mu}$ )- for bundles perpendicular -resp. parallel- to material surface. In the literature, many micrographs show such roughness features on carbon-based composites during ablation by oxidation [9, 10] or both oxidation and sublimation [11, 12, 13, 8]. Due to an important recession of the intra-bundle matrix, fibers, which are less reactive, are partially stripped, become thinner, and acquire a needle shape. The surface roughness of the extra-bundle pitchbased matrix can be neglected at this scale.
- A microscopic surface roughness appears on the fibers and on the extra-bundle matrix. Fiber tips are faceted (micrograph  $a_{\mu}$  and  $c_{\mu}$ ). The extra-bundle pitch-based matrix shows denuded layers arranged in a parallel fashion (micrograph  $b_{\mu}$ ). This is coherent with its pseudo-crystalline anisotropic structure.

X-ray computed microtomography (CMT) has been carried out on a C/C composite after a short oxidation test. The resolution (size of a pixel) is  $0.3\mu m$ . After 3D reconstruction, the agreement between tomographs and SEM micrographs is correct (see figure 3). The resolution of the SEM micrograph is higher than for the tomographs; nevertheless, as illustrated on figure 3 through the numerical extraction of a fiber, the CMT enable 3D quantitative

measurement and analysis of the material structure. This property is used in the section 3 in the evaluation of the size of the "needles".

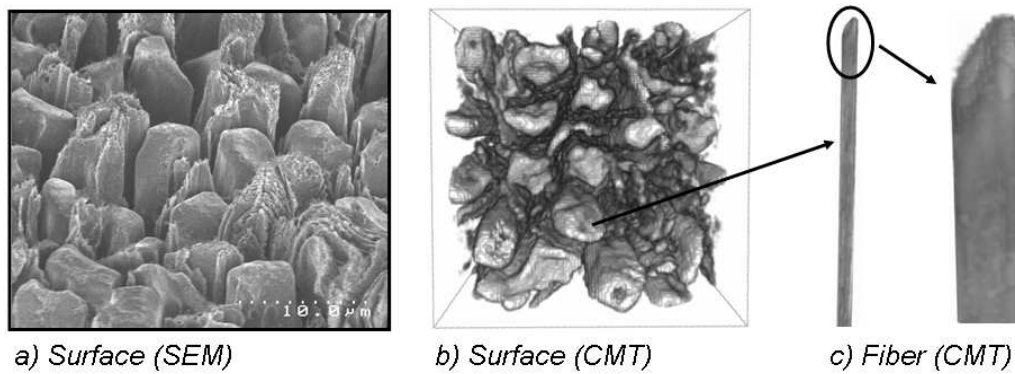


Figure 3. Comparison of SEM and tomography observations of a C/C surface after a short ablation test.

The surface roughness features observed after plasma jet ablation are quite similar to the features described above. The main difference is noted at macroscopic scale where the section of emerging bundles is ogival rather than conical. Indeed, they are smoothed out by advection or thermal gradient [8].

From the above presented descriptions and classifications, it appears that ablation-related geometrical features of the rough surface mainly follow the material structure. Accordingly, it will be called structural roughness to make a difference with a purely physical roughness which has already been observed on homogeneous materials and modeled [2]. This physical roughness consists in scalloped morphologies and is not correlated to material structure [14].

### 2.3. The causes of structural surface roughness

The constituents of ablative carbon-based materials are made of various kinds of turbostratic carbons [15], which differ from graphite by a less organized and extended crystalline structure [16] (see figure 4). At atomic scale, this difference arises from a lack of pure  $sp^2$  carbon atoms, as compared to graphite; this fact might be explained by the presence of  $sp^3$ -like defects [17].  $sp^3$ -like defects tends to disorientate graphene planes inside graphene layers, which can be slightly curved [17] or exhibit an inter-plane average length up to ten percent larger than graphite one [15]. The change of inter-plane average length (X-ray diffraction measurement of  $d_{002}$ ) reduces the local density.  $d_{002}$  generally decreases with graphitization degree [18]. The extension of graphene planes and the size of graphene stacks increase with graphitization degree [16, 18]. Consequently, the local density increases with graphitization degree [15]. The way the graphene stacks are connected together has also a strong effect on density, as it can lead to a more or less optimized space occupation. Then, the size of the representative elementary volume for the global density evaluation is about ten times the size of individual graphene stacks.

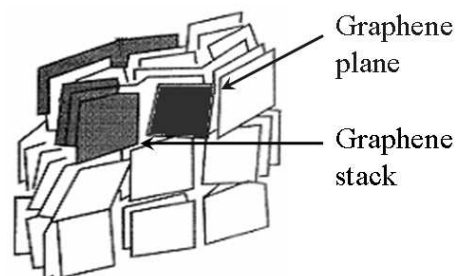


Figure 4. Sketch of the structure of turbostratic carbon [16].

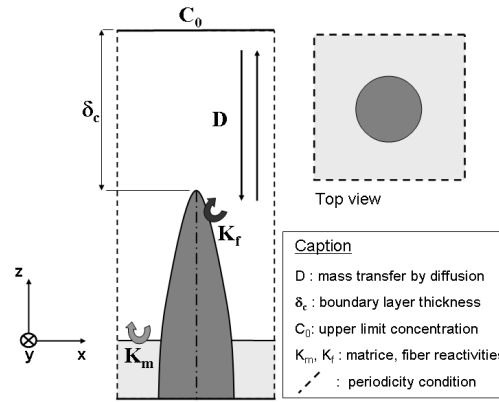


Figure 5. Scheme of the elementary pattern and of the proposed model

The gasification rates (oxidation or sublimation) of the graphene planes increase with plane perimeter to plane surface ratio [19]. Indeed, the reactivity of the edges, whose atomic conformations constitute active sites [20], is three orders of magnitude higher than the reactivity of the surface [21], which contains few defects and then few active sites. It arises that the gasification properties of turbostratic carbons are strengthened with the graphitization rate [1], as graphitization tends to expand the graphene planes. Consequently, the gasification rate of turbostratic carbons generally decreases as local density increases [22]. An interpretation of the graphene plane reactivity followed by a multi-scale modeling of poly-crystalline graphite has produced results in qualitative agreement with the experimental tendencies [23].

The local recession velocity of the surface depends on the local reactivity. This effect leads to the establishment of surface roughness on composite materials, which are heterogeneous materials made of several kinds of turbostratic carbons. This phenomenon can be balanced by a mass transfer limitation in the fluid phase. The competition between mass transfer and heterogeneous reaction can explain a large part of the roughness features observed on the material surface.

### 3. MODELING AND SIMULATION OF MULTI-SCALE SURFACE ROUGHNESS

#### 3.1. C/C composites bundles

The evolution described in section 2.2 of the pointed fibers has been sketched in 2D by Han[12]. We recently succeeded in modeling it in transient regime using a simulation code [8]. The model equations have been solved analytically in steady state [6]. First, the model is presented; then, the results of the analytical solution are summarized and exploited.

As specified in the previous section, the C/C composite bundles are heterogeneous. They are made of fibers and matrix, which are assumed to be homogeneous and isotropic. They are ablated following either a first order oxidation process or sublimation under Knudsen-Langmuir hypotheses. These two cases are mathematically equivalent considering either reactant diffusion to the wall or vaporized carbon diffusion from the wall [2]. The gasification rate of the fibers ( $k_f$ ) is lower than for the matrix ( $k_m$ ).

The proposed model is sketched on figure 5. On this scheme the stationary rough surface is represented; however at initial time, the fluid/solid interface is flat. This profile has therefore to be obtained using a moving fluid/solid interface modeling.

Let us write mass conservation of the reactant (of molar concentration  $C$ ) in the fluid phase:

$$\frac{\partial C}{\partial t} + \nabla \cdot (-D\nabla C) = 0 \quad (1)$$

Boundary conditions relative to the model domain are:

- On boundary layer top:  $C = C_0$ ;
- At the fluid/solid interface the oxidation molar rate  $r$  writes:

$$r = (-D\nabla C) \cdot \mathbf{n} = -k_j C \quad (2)$$

where  $\mathbf{n}$  is the normal to the surface, and  $k_j$  ( $m/s$ ) the reaction kinetic constant of matrix ( $j = m$ ) or fibers ( $j = f$ );

- Periodicity on the lateral boundaries (the bundle section is supposed infinite in transverse directions).

The interface position ( $S(x, y, z, t)$ ) is given by the simultaneous resolution of equations (1-2) and of [2]:

$$\frac{\partial S}{\partial t} + \mathbf{v} \cdot \nabla S = 0 \quad (3)$$

where  $\mathbf{v} = v_s \mathbf{r}\mathbf{n}$  is the surface local normal velocity, with  $v_s$  the solid molar volume.

The resolution of this model in steady state for an axi-symmetric fiber gives the geometry of the fiber after ablation as a function of two dimensionless numbers (figure 7): (i) the Sherwood number ( $Sh = R_f k_f / D$ ), which quantifies the competition between reaction and diffusion, (ii) the reactivity contrast between matrix and fibers ( $A = \frac{k_m v_m}{k_f v_f}$ ) [6]. The model has been validated using independent feeding and validation data [7, 6]. The comparison of the micrographs of figure 2 to the results of the model presented at figure 7 shows that the experimental Sherwood number is low since fibers are conical. This means that ablation is limited by reaction.

Actually, as shown on figure 3, fiber and matrix have the same oxidation rate. However, an interphase of matrix lying between the bulk matrix and the fiber is more reactive [6]. The TEM micrograph of figure 6 shows that the crystallite size is smaller for the interphase matrix than for the bulk matrix. Under the light of the analysis of the turbostratic carbon properties of the section 2.3, this property explains the higher oxidation rate of the interphase. The model presented above still works when interphase is included. Using this model and qualitative measurement of the needle size ( $100 \mu m$ ) using tomographs, the interphase to fiber oxidation rate ratio  $A$  has been evaluated [6]. It lies around 30. The reactivity of PAN graphitized fibers has been evaluated independently in the same oxidation conditions:  $k_f \simeq 10^{-5} m/s$  [7]. According to the model, the yarn obeys a weakest-link rule as ablation is limited by reaction: its effective reactivity is equal to the interphase reactivity [6]. The fiber surface  $S_f$  increases until the following relation is respected:  $S_f k_f = S_p k_i$ , where  $S_p$  is the projected surface of the fiber.

The case of bundles parallel to surface is quite difficult to cope with. The model presented above is not appropriate to model it. To predict the effective reactivity, one has to take into account diffusion into porous media. The effective reactivity can be higher than the highest reactivity of the components of the composite. There are at least three ways to evaluate the effective reactivity. (i) The effective reactivity can be approximated by a simple 2D analytical model. The main difficulty is to evaluate the tortuosity for gas diffusion through the bundles. An evaluation of the tortuosity could be done through an analysis of ablated bundles and a percolation analysis [24]. (ii) An other way is to carry out direct numerical simulations of ablation using a reaction-diffusion code [6]. The input data are the oxidation rates of the bundle components evaluated on the perpendicular bundles. (iii) A last way consists in deducing the effective reactivity by an inverse analysis. The method is quite similar to the method used to evaluate the interphase oxidation rate. First, a parametrical study on the model of the composite scale is processed. Then, the comparison of the simulations results to the morphologies experimentally observed should provide the effective reactivity of the parallel bundles.

In this work, the third way has been selected. Then the first step is to model the ablation behavior of the C/C composite.

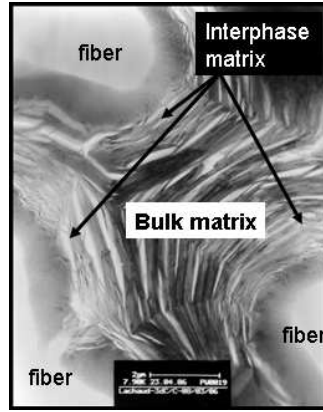


Figure 6. TEM micrograph of the C/C bundle texture (P. Weisbecker, M. Alrivie)

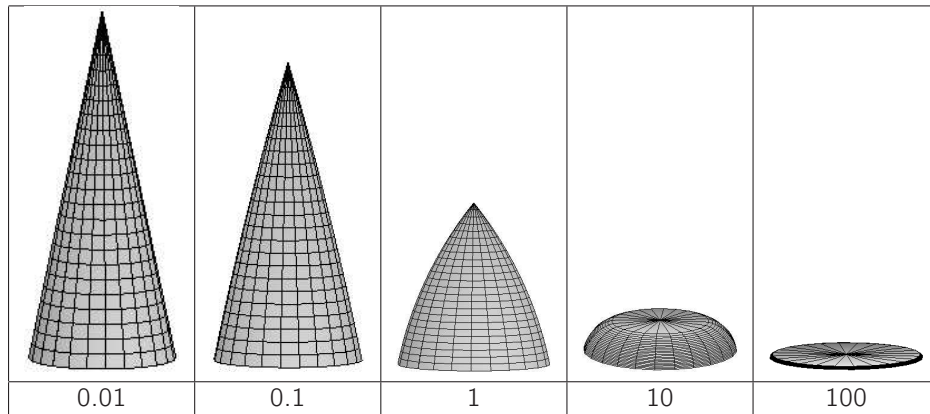


Figure 7. Fiber morphology at steady state as a function of  $Sh$  (with  $A = 5$ ).

### 3.2. C/C composites

In the oxidation reactor, it has been shown that advection and thermal gradients could be neglected [7]. Hence, the model presented above can be applied to a square-section bundle perpendicular to the surface and surrounded by a more reactive phase: either inter-bundle matrix or parallel bundles (see figure 2). In a first approach, the perpendicular bundle is considered to be surrounded by a single phase assumed flat and smooth. The equation of the surface  $z = S(x, y)$  in steady state is easily inferred from [6]. In cartesian coordinates, it writes:

$$\text{if } |x| > |y| \quad z = f(x) \quad \text{else } z = f(y) \quad \text{with } (x, y) \in [-l, l]^2 \quad (4)$$

where

$$f(u) = La \left( \sqrt{A^2 - \left( (|u| - l)/La + \sqrt{A^2 - 1} \right)^2} - 1 \right) \quad (5)$$

with  $La = D/k_b$ , a length, and  $l$  a half of the length of an edge of the square section of the bundle. According to this model, the perpendicular bundles should emerge from the weak phase surface and adopt a pyramidal geometry if diffusion phenomenon is not limiting, *i. e.* Sherwood number is not large (see figure 8).

To model accurately the composite behavior, its actual architecture has to be taken into account. A numerical unit cell has been designed as sketched on figure 9-a. To solve this problem in 3-D and in non-stationary regime, an efficient numerical simulation code, named AMA, has been developed on a Monte-Carlo random-walk principle. AMA, which is a C ANSI implementation, contains four main parts. (i) A 3-D image containing several phases

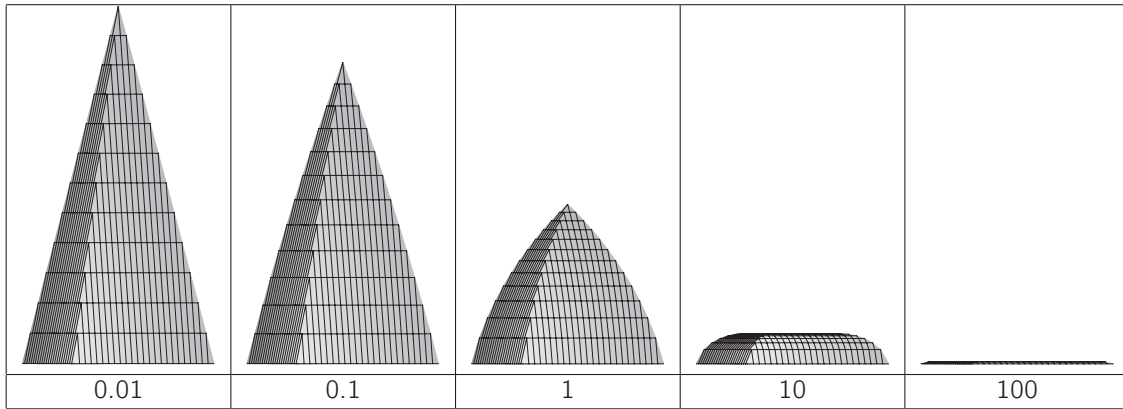


Figure 8. Bundles morphology at steady state as a function of  $Sh$  (with  $A = 5$ ).

(fluid/solids) is described by discrete cubic voxels method. (ii) The moving fluid/solid interface is determined by a simplified marching cube approach [25]. (iii) Mass transfer by diffusion is simulated by a Brownian motion simulation technique [24], which is a continuum (grid-free) and rapidly converging method to simulate diffusion in a continuous fluid. (iv) Heterogeneous first order reaction on the wall is simulated by a sticking probability ( $\tilde{P}$ ) adapted to the Brownian motion simulation technique [8]. AMA has been validated by comparison to a 1D analytical model in transient regime [8] and to the axi-symmetrical model presented above in steady state [6].

The oxidation rate of the perpendicular bundles is deduced from the first change of scale ( $k_{b,perp} = 3 \cdot 10^{-4} \text{ m/s}$ ). In this case, the Sherwood number is large. The reactivity of the inter-bundle matrix has been evaluated independently in the same oxidation conditions. The reactivity contrast between bundles and inter-bundle matrix  $A$  has been found to be equal to 3. As introduced in the previous subsection, the effective reactivity of the parallel bundles  $k_{b,para}$  is evaluated by a parametrical study on  $k_{b,para}$ . The adequate reactivity is obtained when the simulation results are in quantitative agreement with the experimental morphologies. Using this inverse method, the perpendicular bundles to parallel bundles reactivity ratio is estimated to lie around 4. The simulation of the surface roughness onset, for the values of reactivity cited above, is presented on figure 9. At the beginning of the simulation, the surface is flat (figure 9-a). Then, as expected, the perpendicular bundles progressively emerge from the surface (figure 9-b) and their morphology becomes almost pyramidal (figure 9-c). When the contrast between the two weak phases is high, the pyramids do not appear perfect but distorted. The surface of the parallel bundles is slightly undulated as noticed in subsection 2.2 for ablated materials. The similarity of figure 9-b with figure 2-M supports the conclusions that (i) the model is adequate, (ii) the steady state has not been reached at the end of the experiment, and (iii) the reactivity values of the simulation are adequate.

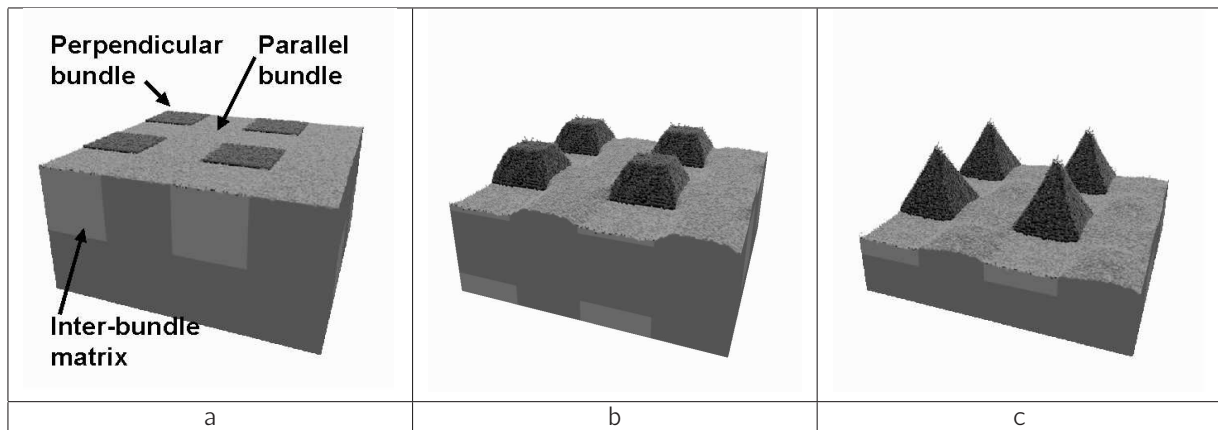


Figure 9. C/C composite ablation simulation- a) numerical cell before ablation, b) transient regime, and c) steady state

## 4. CONCLUDING REMARKS

In this work, the surface roughness onset of C/C composites during ablation in an oxidation reactor has been studied and modeled. First, a microscopic analysis, using SEM, CMT, and TEM, has shown that the surface roughness was strongly correlated to the turbostratic carbon structure and to the multi-scale architecture of the composite. The heterogeneity of the composite with respect to heterogeneous mass transfer has been assumed to be the cause of the onset of surface roughness. Accordingly, the proposed models are based on the simultaneous resolution of a gas diffusion-reaction equation and of a surface evolution equation.

The surface roughness onset has been modeled using two changes of scales : (i) microscopic scale (fiber, intra-bundle matrix) to mesoscopic scale (bundle) and (ii) mesoscopic scale (bundle, inter-bundle matrix) to macroscopic (composite) scale. First, using the results of a previous work, the ablation behavior of the perpendicular bundles is modeled in steady state to infer its effective behavior. Then, the overall composite structure is modeled in 3D in transient regime. The input values are evaluated by three complementary ways: (i) experimental (inter-bundle matrix), (ii) deduced from the first change of scale (perpendicular yarn), and (iii) obtained by identification using an inverse method (parallel yarn). At each scale, the models have been validated by comparison to experiments in an oxidation reactor.

Many perspectives arise from this study:

- The results of the models can help understand ablation of C/C composites in real flight experiments, at least from the material point of view. Indeed, they prove that from the study of the surface morphology, it is possible to deduce by inverse analysis the properties of the elements in the test conditions. For instance, since advection and thermal gradients are always negligible at mesoscopic scale, the results of this work could be rigorously applied to infer the properties of the bundle components by a morphological analysis of any ablated C/C composite.
- An exploitation in terms of guidelines for material optimization is at hand : it should be possible to use the presented multi-scale model to look for composites with less pronounced roughness and/or equivalent reactivities.
- AMA, the modeling simulation code implemented for this study, has to be coupled to a Navier-Stokes solver to predict efficiently the onset of surface roughness at macroscopic scale for real flight experiments. It could be the purpose of future collaborations between ARA members.

## ACKNOWLEDGMENTS

The authors wish to thank P. Weisbecker for taking and scanning the MET micrograph and M. Alrivie for the preparation of the adequate thin sample. The authors also wish to thank CNRS and CEA for Ph. D. grant to J. Lachaud.

## REFERENCES

- [1] L. M. Manocha and E. Fitzer. *Carbon reinforcement and C/C composites*. Springer, 1998.
- [2] G. Duffa, G. L. Vignoles, J.-M. Goyh n che, and Y. Aspa. Ablation of C/C composites : investigation of roughness set-up from heterogeneous reactions. *International Journal of Heat and Mass Transfer*, 48(16):3387–3401, June 2005.
- [3] M. R. Wool. Summary of experimental and analytical results. Technical Report SAMSO-TR-74-86, Passive Noretip Technology Program (PANT), January 1975.
- [4] J. Couzi, J. de Winne, and B. Leroy. Improvements in ablation predictions for reentry vehicle nosetip. In *Proceedings of the third European symposium on aerothermodynamics for space vehicles*, pages 493–499, ESA, Noordwijk, The Netherlands, 24–26 November 1998.

- [5] J. A. Keenan and G. V. Candler. Simulation of ablation in earth atmospheric entry. In AIAA Paper, editor, *AIAA 28th Thermophysics conference*, volume 93, Orlando, FL, July 1993.
- [6] J. Lachaud, Y. Aspa, G. Vignoles, and G. Bourget. Experimental characterization and 3D modelling of carbon/carbon composites oxidation : role of the interphase. In *12<sup>th</sup> European Conference on Composite Materials*, Biarritz, France, 1-3 September 2006. 8 p. To appear.
- [7] N. Bertrand, J. Lachaud, G. Bourget, F. Rebillat, and G. L. Vignoles. Identification of intrinsic carbon fiber oxidation kinetics from experimental data and CFD modeling. In *12<sup>th</sup> European Conference on Composite Materials*, Biarritz, France, 1-3 September 2006. 8 p. To appear.
- [8] J. Lachaud, G. L. Vignoles, J. M. Goyh n che, and J. F. Epherre. Ablation in C/C composites: microscopic observations and 3D numerical simulation of surface roughness evolution. In L. P. Cook, editor, *Thermochemistry and Metrology of Interfaces*, volume 191 of *Ceramic Transactions*, page 12. American Ceramic Society, 2006. 12 p. To appear.
- [9] D. Cho, J. Y. Lee, and B. I. Yoon. Microscopic observations of the ablation behaviours of carbon fibre/phenolic composites. *Journal of Materials Science Letters*, 12:1894–1896, 1993.
- [10] E. Duvivier. *Cin tique d'oxydation d'un composite carbone/carbone et influence sur le comportement m canique*. PhD thesis n 1692, Universit  de Bordeaux I, 1997.
- [11] D. Cho and B. I. Yoon. Microstructural interpretation of the effect of various matrices on the ablation properties of carbon-fiber-reinforced composites. *Composites science and technology*, 61:271–280, 2001.
- [12] J. C. Han, X. D. He, and S. Y. Du. Oxidation and ablation of 3D carbon-carbon composite at up to 3000 C. *Carbon*, 33(4):473–478, 1995.
- [13] Y.-J. Lee and H. J. Joo. Investigation on ablation behavior of CFRC composites prepared at different pressures. *Composites: Part A*, 35:1285–1290, 2004.
- [14] G. Vignoles, Y. Aspa, J. Lachaud, G. Duffa, J. M. Goyheneche, J. F. Epherre, N. T. H. Nguyen-Bui, M. Quintard, and B. Dubroca. Multiscale study of ablation in carbon/carbon composites : Surface roughness evolution and possible physicochemical causes. In *ESA Workshop on Ablation, ESTEC*, Noordwijk, The Netherlands, 13 Oct 2005.
- [15] C. Sauder. *Relation microstructure/propri t s   haute temp rature dans les fibres et matrices de carbone*. PhD thesis n 2477, Universit  Bordeaux 1, 2001.
- [16] X. Bourrat. *Sciences of carbon materials*, chapter 1. Structure in carbons and carbon artifacts, pages 1–97. Universidad de Alicante, 2000.
- [17] J-M. Vallerot, X. Bourrat, A. Mouchon, and G. Chollon. Quantitative structural and textural assessment of laminar pyrocarbons through raman spectroscopy, electron diffraction and few other techniques. *Carbon*, 44(9):1833–1844, 2006.
- [18] A. Oberlin, J. Goma, and J. N. Rouzaud. Techniques d' tude des structures et texture (microtextures) des mat riaux carbon s. *J. Chimie Physique*, 81(11/12):701–710, 1984.
- [19] J. B. Donnet. Structure and reactivity of carbons: from carbon black to carbon composites. In *15th Biennial conference on carbon*, Philadelphia, PE, June 1981.
- [20] E. J. Hippo. The role of active sites in the inhibition of gas-carbon reactions. *Carbon*, 27(5):689–695, 1989.
- [21] G. H. Hennig. Anisotropic reactivities of graphite - I. Reaction of ozone and graphite. *Carbon*, 3(2):107–108, 1965.
- [22] P. Delhaes. *Le carbone dans tous ses  tats*, chapter 1. Le polymorphisme des solides carbon s, pages 1–118. Gordon and Breach Science Publishers, 1997.
- [23] J. Lachaud, Y. Aspa, G. Vignoles, and J.-M. Goyh n che. 3D modeling of thermochemical ablation in carbon-based materials: effect of anisotropy on surface roughness onset. In M. Dinguirard, editor, *10<sup>th</sup> International Symposium on Materials in a Space Environment*, volume 72, Collioure, France, June 2006. ONERA. 10 p. To appear.
- [24] S. Torquato and I. Kim. Efficient simulation technique to compute effective properties of heterogeneous media. *Appl. Phys. Lett.*, 55:1847–1849, 1989.
- [25] G. L. Vignoles. Modelling binary, Knudsen, and transition regime diffusion inside complex porous media. *J. Phys. IV France*, C5:159–166, 1995.